IEEE Access
The journal for rapid open access publishing

Received June 27, 2014, accepted August 11, 2014, date of publication August 21, 2014, date of current version September 4, 2014.

Digital Object Identifier 10.1109/ACCESS.2014.2350531

Continuous Electrowetting of Non-toxic Liquid Metal for RF Applications

RYAN C. GOUGH, (Student Member, IEEE), ANDY M. MORISHITA, (Student Member, IEEE), JONATHAN H. DANG, (Student Member, IEEE), WENQI HU, (Student Member, IEEE), WAYNE A. SHIROMA, (Senior Member, IEEE), AND AARON T. OHTA, (Member, IEEE)

Department of Electrical Engineering, University of Hawai'i at Mānoa, Honolulu, HI 96822 USA

Corresponding author: R. C. Gough (rgough@hawaii.edu)

This work was supported in part by the National Science Foundation under Grant ECCS-1101936 and in part by the National Consortium for Measures and Signatures Intelligence Research.

ABSTRACT Continuous electrowetting (CEW) is demonstrated to be an effective actuation mechanism for reconfigurable radio frequency (RF) devices that use non-toxic liquid-metal tuning elements. Previous research has shown CEW is an efficient means of electrically inducing motion in a liquid-metal slug, but precise control of the slug's position within fluidic channels has not been demonstrated. Here, the precise positioning of liquid-metal slugs is achieved using CEW actuation in conjunction with channels designed to minimize the liquid-metal surface energy at discrete locations. This approach leverages the high surface tension of liquid metal to control its resting position with submillimeter accuracy. The CEW actuation and fluidic channel design were optimized to create reconfigurable RF devices. In addition, solutions for the reliable actuation of a gallium-based, non-toxic liquid-metal alloy (Galinstan) are presented that mitigate the tendency of the alloy to form a surface oxide layer capable of wetting to the channel walls, inhibiting motion. A reconfigurable slot antenna utilizing these techniques to achieve a 15.2% tunable frequency bandwidth is demonstrated.

INDEX TERMS Aperture antenna, electrowetting, frequency-reconfigurable, liquid metal, reconfigurable antenna, slot antenna.

I. INTRODUCTION

Reconfigurable radio-frequency (RF) devices are capable of dynamically optimizing performance to achieve multiple, and oftentimes conflicting, design criteria. For example, such a device may be able to achieve the noise-cancelling benefits of a narrow-band frequency response while also supporting multiple frequency channels across a wide bandwidth. This optimization is normally accomplished by adjusting the device's frequency response using electrically variable reactive elements. Varactors [1], [2] and PIN diodes [3], [4] are popular choices due to their low-power operation, small size, and low cost. Microelectromechanical systems (MEMS) have also proven to be an effective solution, allowing a greater range of device flexibility and at increasingly lower activation voltages [5], [6].

Recently, interest has grown in using liquid metal to create reconfigurable devices. A fluidic conductor avoids the nonlinearity of semiconductor components, and can be dynamically deformed and shifted to achieve different performance criteria. Liquid-metal elements are also capable of retaining these physical changes after the actuation signal is removed, as opposed to MEMS devices, which often require a continuous actuation voltage to maintain non-baseline performance states [5], [6]. The development of liquid-metal devices has been hampered in the past by the high toxicity of mercury, the only naturally occurring metal that exists as a liquid at room temperature. However, a non-toxic liquid-metal alloy called Galinstan (composed of 68.5% gallium, 21.5% indium, and 10.0% tin) [7] has become available on the commercial market, opening the door to the use of liquid metal without the health concerns presented by mercury. Galinstan has a high conductivity (2.30×10^6 S/m) and is a stable liquid across a wide temperature range (-19 to 1300 °C) [7], making it a suitable substitute for mercury in most RF applications.

A wide variety of reconfigurable RF devices have already been designed using Galinstan and similar non-toxic gallium-based alloys [8]–[16]. However, these devices largely use hydraulic pressure as their actuation mechanism, requiring pumps for commercial implementation. Electrowetting on dielectric (EWOD) has been used successfully, but EWOD devices often require high actuation voltages that

must be continuously applied to maintain the liquid metal deformation necessary for adjustable performance [14], [17].

Continuous electrowetting (CEW) is another technique that has been used to create a wide variety of micro-scale devices [18]–[20]. CEW actuation electrically induces a surface-tension gradient along the length of a liquid-metal slug submerged in an electrolyte, creating Marangoni forces along the liquid-liquid interface and inducing motion of the slug [21]. The mechanics of CEW are detailed in [18], [21], and [22], although in all of these cases the authors use a mercury slug submerged in sulfuric acid. Unlike mercury, Galinstan and most gallium-based alloys develop surface oxidation in the presence of even small amounts of oxygen [7]. This oxide layer can inhibit the formation of any surface tension gradient, impeding and often preventing motion by CEW. Thus, conventional CEW actuation techniques are not immediately transferable to Galinstan-based devices.

Immersing Galinstan in a strong acid or base can help to reduce this oxide, but recent research has shown that a DC potential applied across the electrolyte, a necessary condition for CEW, allows the oxide to re-form and inhibit motion [23]. Furthermore, controlling the position of a high-density liquid-metal slug in a low-friction environment can be challenging, so most CEW applications either require that the slug move from one extreme of the channel to the other [19], [20], or purposefully trap the slug to take advantage of the resulting pumping effect on the electrolyte [24].

This paper discusses the challenges of using CEW as an actuation mechanism for controlling a non-toxic liquid-metal alloy (Galinstan) as a tuning element in an RF device. Solutions for the reliable actuation and high-fidelity position control of a Galinstan slug immersed in an alkaline carrier fluid are presented, and a prototype device utilizing the discussed solutions to achieve a reconfigurable frequency response is demonstrated.

II. THEORY OF OPERATION

A. CONTINUOUS ELECTROWETTING FOR LIQUID-METAL ACTUATION

When a liquid-metal droplet is submerged in an electrolytic solution, an electrical double layer (EDL) forms at the interface of the two liquids [18]. The charge distribution of the EDL influences the surface tension at the interface as described by the integrated Young-Lippman equation:

$$\gamma = \gamma_o - \frac{C}{2}(V - V_o)^2, \tag{1}$$

where γ is the surface tension of the liquid metal, γ_o is the intrinsic surface tension in the absence of the EDL, C is the per-unit capacitance across the EDL, V_o is the intrinsic voltage across the EDL, and V is an externally applied voltage [18]. This surface tension, in turn, can describe the pressure differential across the droplet-electrolyte interface at each end of the slug via the Young-Laplace equation:

$$p = \gamma\left(\frac{1}{R_1} + \frac{1}{R_2}\right), \tag{2}$$

where p is the pressure differential, γ is the surface tension, and R_1 and R_2 are the radii of curvature at each meniscus [22].

By applying a voltage across the electrolyte, a potential gradient is developed along the length of the liquid-metal slug, breaking the inherent symmetry of the EDL charge distribution and creating a corresponding gradient in the surface tension of the liquid metal as described by (1). The surface tension will be lower where the relative voltage across the EDL is higher, which for a liquid-metal slug immersed in an alkaline solution will be at the cathode end [23]. This results in a lower pressure drop from the liquid metal to the electrolyte at the cathode end relative to the anode as described by (2), and this pressure imbalance results in the net motion of the slug in the direction of its cathode end (toward the positive electrode) [22].

This effect, in which a slug in an electrolyte-filled channel 'wets' in a given direction due to an electrically controlled surface-tension imbalance, is known as continuous electrowetting (CEW) and has been used for MEMS pumping [19] and micro-motor [18] applications, as well as for optical switching [20]. Recently, researchers have also utilized the pressure imbalance caused by electrically manipulating the surface tension of a captive liquid-metal droplet to perform macro-scale pumping of an electrolyte [24].

The surface-tension-based motion mechanism described here is in contrast to conventional electrowetting techniques such as EWOD, where the liquid wetting is electromechanical in nature and driven by electrostatic force [25], [26]. This means that EWOD motion can be applied to liquids as well as to conductive solids in a low-friction environment [25], [26]. This is not the case for CEW, and efforts made to reproduce CEW motion with different conductive solids by both our team and others [23] have been unsuccessful. Similarly, our efforts to reproduce the strong pumping effect of a captive liquid-metal droplet undergoing CEW actuation seen in [24] with conductive solids have also failed. For these reasons we believe that the CEW actuation mechanism is indeed the result of surface tension manipulation, and as such is distinct from conventional electrowetting.

B. LIMITING FACTORS FOR RF INTEGRATION

Early MEMS experiments with CEW have almost always used mercury as the liquid metal, normally submerged in an acidic solution such as H_2SO_4 [18], [20]–[22]. While this allowed researchers to study the effects and potential advantages of CEW, the combination of a toxic liquid metal immersed in a highly corrosive acid can limit the commercial feasibility of the resulting devices.

The introduction of non-toxic, gallium-based alloys such as Galinstan alleviates much of this health concern, but Galinstan readily oxidizes in the presence of oxygen levels greater than 1 ppm [7]. This oxide layer, which Raman measurements indicate is likely β-Ga_2O_3 [23], acts as a 'skin' on the surface of the liquid metal and prevents it from behaving as a classical liquid. In addition, while Galinstan itself is largely non-wetting, the β-Ga_2O_3 oxide layer will

wet to a wide variety of surfaces, leaving behind a residue that can limit device usability. Thus, in many applications utilizing Galinstan this oxide residue must be periodically removed [27]. In CEW applications the droplet is normally immersed in an electrolyte that can reduce this oxide layer, such as HCl or NaOH [23]. However, it has recently been shown that applying a potential gradient across the electrolyte leads to the reformation of the oxide on the anode end of the droplet [23]. Once re-formed, this oxide can adhere to the walls of the enclosing channel and prevent droplet motion if the CEW-induced pressure is smaller than the internal cohesion of the droplet, or cause the droplet to split if the external pressure exceeds internal cohesion. In either case, motion of the droplet is effectively halted.

In addition, past experiments with CEW have been limited to applications where the liquid-metal slug is expected to travel the entirety of the channel [20], or where the slug is purposefully trapped with the goal of utilizing this blockage to create electrolytic pumping [24]. These operational limits are necessary because it can be difficult to control the slug's position within the channel due to the low-friction environment, as the high-density Galinstan slug (6440 kg/m^3 [7]) contains enough mass for inertia to become a significant factor in its deceleration. The slug's motion can also create a pressure differential within the electrolyte on either end of the slug, and once actuation is discontinued this pressure differential can be strong enough to displace the slug from its intended position. For RF applications in which the slug is intended to act as a dynamic part of the signal waveguide, it is important to be able to control the slug's incremental position within the channel to a high degree of accuracy.

III. ADAPTATIONS FOR RF IMPLEMENTATION

As identified in the previous section, the two most significant challenges in integrating CEW actuation of a non-toxic liquid metal such as Galinstan in a closed-channel system are reliable actuation and positioning. Each of these issues, along with the implemented solutions, will be discussed in the following sections.

A. ACTUATION

Fig. 1 shows top-down, high-speed camera images of a Galinstan slug undergoing CEW actuation in a closed rectangular channel that is 2 mm wide, 600 μm high, and 40 mm long. Prior to electrical actuation, this slug is able to move freely throughout the channel. When a 7-VDC potential is applied across the electrolyte, the slug begins moving toward the positive probe (toward the right in Fig. 1a), but within 15 ms the anode of the slug becomes 'stuck' and will no longer move forward. At 360 ms after actuation, a state of equilibrium is reached in which the pull on the cathode towards the positive probe is balanced by the internal cohesion of the liquid metal pulling back toward the fixed anode, and the now-elongated slug remains stationary (Fig. 1c). Once the actuation voltage is removed, the slug contracts toward the anode, but is soon once again able to move freely; in Fig. 1f it

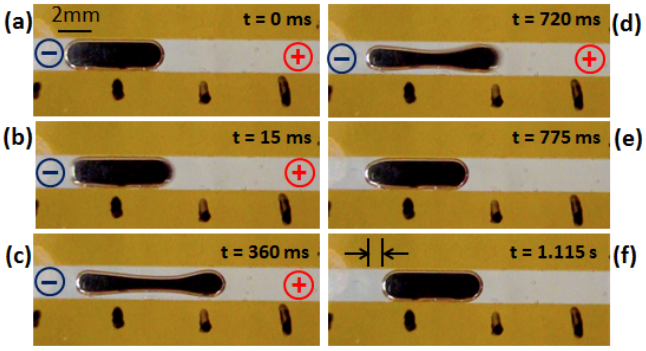

FIGURE 1. Liquid-metal slug in a closed channel with 7-VDC CEW actuation. Upon actuation (a), the slug begins moving from left to right until the newly oxidized anode wets to the sides of the channel (b). The cathode continues to be pulled forward until reaching an equilibrium (c). Once the voltage is removed (d), the slug contracts back towards the anode (e) and is soon able to move freely once the oxide on the anode has been reduced (f).

has already been pushed slightly to the right by the pressure imbalance of the electrolyte after contraction. This is strong evidence that the obstruction that halted the slug's forward movement was the result of oxide regrowth, caused by the application of a potential across the electrolyte, and not due to other factors, such as debris in the channel.

To overcome the problem presented by oxide regrowth, the DC actuation signal is replaced by a DC-offset square wave at a frequency of 20 to 30 Hz. Replacing the DC signal with a square wave allows for continuous motion in a closed channel through a two-part process that repeats with each cycle. When the signal is 'high', conditions in the channel resemble those of conventional CEW actuation and the droplet is pulled toward the positive probe while the anode begins to re-oxidize. When the signal is 'low', the polarity in the channel has been reversed, hastening the reduction of the oxide layer on the (former) anode in time for the beginning of the next signal period. In this manner the slug alternates between being pulled forward and having its anode continually reduced. The asymmetry provided by the DC offset determines the direction of net movement for the slug.

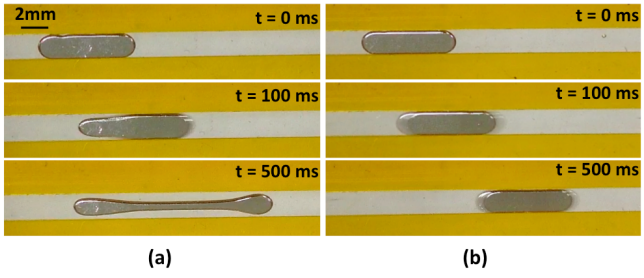

FIGURE 2. CEW in a 2-mm-wide, 400-μm-high rectangular channel with (a) 8 VDC and (b) square-wave actuation. Square-wave signal parameters are 8 Vpp, +3 VDC offset, and 30 Hz.

Fig. 2 shows a top view of a liquid-metal slug in a rectangular channel with a width of 2 mm and a height of 400 μm.

The slug is actuated once with an 8-VDC signal (Fig 2a) and then again with a 30-Hz, 8-V_{pp} square wave with a +3 VDC offset (Fig. 2b). With the DC signal alone, the trailing edge of the slug oxidizes and the slug's motion is halted within the first 100 ms, similar to what was previously observed in Fig. 1. Square-wave actuation, however, continuously reduces the oxide on the trailing edge and allows for smooth motion throughout the channel.

In [24] it was reported that pumping of the surrounding electrolyte by a captive Galinstan droplet was maximized by applying a square-wave actuation signal with an offset voltage V_{off} equal to half the peak-to-peak voltage V_{pp}. However, to achieve smooth motion of a Galinstan slug, the DC offset must fall within $0 < |V_{off}| < V_{pp}/2$. In other words, some polarity change in the channel is required. This is because there is insufficient time between cycles for the electrolyte to completely reduce the newly formed oxide layer on its own; by 'pulling' the slug in the opposite direction, Marangoni forces along the liquid-liquid interface pump the electrolyte between the slug and the channel walls where wetting has occurred, hastening the oxide reduction and acting as a barrier to prevent future wetting. The net speed of the slug is maximized by keeping the 'low' portion of the period sufficiently close to 0 V to avoid pulling the slug too far backwards, but far enough from 0 V to achieve the desired chemical reduction. Empirically this level has been found to be between −1.0 V and −0.5 V.

B. POSITIONING

The low-friction environment experienced by the liquid-metal slug can present difficulties if the final position of the slug in the channel is to be controlled to a high degree of fidelity. One method for limiting unintended slug displacement is to increase the surface area of the liquid metal relative to its volume, which in turn increases the friction experienced by the slug. Our experiments have shown that for a constant channel width of 2 mm, a channel height of 600 μm can result in the slug being displaced up to 5 mm after the actuation signal is discontinued, but when the height is reduced to 200 μm the displacement is reduced to 1 to 2 mm. While somewhat effective, reducing the channel height also makes it more difficult to actuate the slug. In addition, 1 to 2 mm of uncertainty in the slug's position is still an unacceptable margin of error for many applications.

To obtain more precision in the slug positioning, the high surface tension of Galinstan can be utilized. This can be done by providing the slug with localized points within the channel where it can minimize its surface energy, as first demonstrated in [28]. The surface tension of oxide-free Galinstan in a nitrogen environment has been measured at approximately 535 mN/m [7], although this number is probably slightly lower when Galinstan is immersed in an electrolytic solution [29]. This high surface tension makes the liquid metal sensitive to variations in channel geometry, as these directly affect the surface area of the slug, and thus its free surface energy.

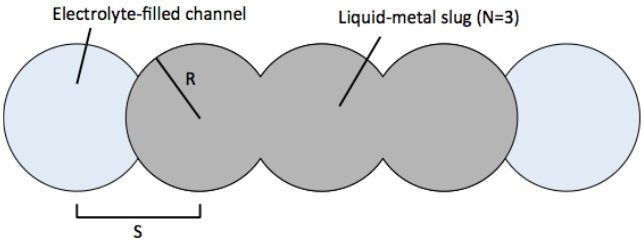

FIGURE 3. Top-view illustration of liquid-metal slug in a channel of interlocking circular chambers. Each chamber has a uniform radius R and is kept at a constant spacing S. The slug's length is given by N, the number of consecutive circular chambers it fills.

Specialized fluidic channels were fabricated to take advantage of Galinstan's high surface tension. Instead of a uniform channel cross-section, a channel made with a series of interlocking circular chambers was used (Fig. 3). These circular chambers act as local minima of surface energy for the liquid metal. Once the CEW actuation signal has been removed, the slug's strong internal cohesion forces it into the nearest of these energy minima. Thus, the channel is divided into a finite number of discrete, overlapping locations in which the slug is able to rest post-actuation, increasing the accuracy of its resting position.

Liquid metal, like all liquids, will seek to minimize its free surface energy by minimizing its surface area [30]. For a liquid-metal slug of finite volume in a closed channel whose height is constant, it is intuitive that the surface area in contact with the floor and ceiling will always remain constant. It follows that so long as the width and length of the channel are much greater than its height, the slug can be approximated as a 2D object of constant area. Thus, the minimization of the liquid metal's surface area can be closely approximated as a minimization of its 2D perimeter. The optimal case is a circle, since this perimeter is the minimum possible for a given area.

An illustration of a liquid-metal slug in a channel of interlocking circular chambers of uniform height is shown in Fig. 3. The slug's volume is assumed to fill N chambers exactly, and if the chambers have identical radii and separation distance the slug's 2D area can be defined as

$$A = N\pi R^2 - 2(N-1)\left[R^2\cos^{-1}\left(\frac{S}{2R}\right) - \frac{S}{4}\sqrt{4R^2 - S^2}\right], \tag{3}$$

where N is the total number of adjacent chambers filled, R is the radius of each circular chamber, and S is the center-to-center distance between adjacent chambers. As discussed, this area will remain constant so long as the channel height remains constant.

The total perimeter for a slug with an area A as described by (3) for any position x within the channel can then be written as

$$P = P(x)_{edge} + (N-1)\left(2\pi R - 4R\cos^{-1}\left(\frac{S}{2R}\right)\right), \tag{4}$$

where $P(x)_{edge}$ is the combined perimeter of the partially filled chambers at each end of the slug. This length will vary

depending on the slug's position, whereas the perimeter of the $N-1$ central chambers will not, as they are always filled regardless of the slug position. Using (4), the change in the slug's perimeter, and thus its surface energy, can be quantified by examining the change in the combined perimeter of the partially filled chambers at the ends of the slug. Furthermore, due to the periodic nature of the circular chambers, we can describe this change for all positions in the channel by investigating the change as the slug moves from one baseline position (N adjacent chambers completely filled) to the next.

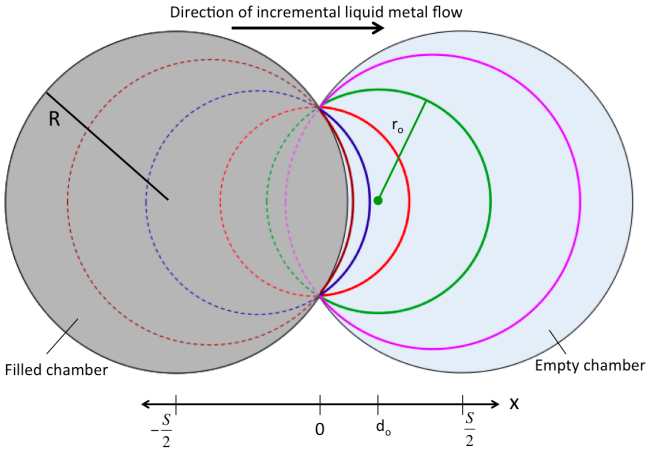

FIGURE 4. The leading edge of the liquid-metal slug moving between circular chambers can be modeled as a series of overlapping circles, from which the changing length of the leading-edge arc can be calculated.

In each of the partially filled chambers at the leading and trailing edge of the slug, the liquid metal will minimize its surface energy by contracting into the smallest possible area. This means the movement of the liquid metal as it fills or recedes from a chamber can be modeled as the movement of a series of overlapping circles, as illustrated for the leading-edge case in Fig. 4. The radius r of each of these circles will vary as a function of both the channel geometry as well as the distance d from the circle's center to the halfway point between the two chambers:

$$r = \sqrt{d^2 + R^2 - \frac{S^2}{4}}. \tag{5}$$

Once r is known for a leading-edge circle at a given distance d from the midpoint between the two chambers, both the changing length of the leading-edge arc as well as the area of the liquid metal now occupying the new chamber can be calculated. If the finite volume of the liquid metal initially fills exactly N chambers, this area can be used to find the area of liquid metal remaining in the trailing-edge chamber, as the sum of the area occupied by the liquid metal in the leading and trailing edge chambers will always equal πR^2. This in turn can be used to relate d and r for the circle describing the trailing-edge arc through the integral:

$$\int_{-r}^{d} \sqrt{r^2 - x^2}\, dx = \frac{d}{2}\sqrt{r^2 - d^2} + \frac{r^2}{2}\tan^{-1}\left(\frac{d}{\sqrt{r^2 - d^2}}\right) + \frac{\pi r^2}{4} = \frac{1}{2}A_{Tr}, \tag{6}$$

where A_{Tr} is the area of the liquid metal in the trailing-edge chamber. In conjunction with (5), the radius and location of the circle describing the trailing edge can now be calculated, and the length of the arc in the trailing-edge chamber determined.

To check the accuracy of this motion model, a MATLAB simulation of a liquid-metal slug filling two chambers ($N = 2$) was performed as the slug moved along a channel for one period. Simulated images predicting the slug's changing shape were compared to video of a similar slug moving through a channel of identical dimensions under CEW actuation. The results demonstrate an excellent fit between the predicted and actual distortion of the liquid metal for different positions within the channel (Fig. 5).

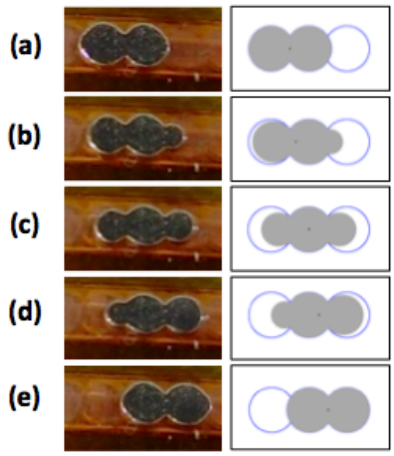

FIGURE 5. A liquid-metal slug ($N = 2$) moving from left to right. The images on the left side are photos as the liquid metal moves in a channel. Corresponding results from a MATLAB simulation are shown on the right. The shape of the liquid-metal slug in the experimental and simulated results match closely.

A plot of the normalized surface energy for a one-chamber ($N = 1$) liquid-metal slug as a function of the position of its center of mass (CoM) as it moves from one chamber to the next is shown in Fig. 6. As expected, the surface energy is at a minimum when the liquid metal fills the circular chamber and reaches a peak halfway between adjacent chambers. This peak varies as a function of channel geometry; lower chamber diameter-to-spacing ratios result in narrower channel passages and increased surface energy peaks, while larger ratios more closely resemble a channel of uniform width and require less additional surface energy for liquid metal displacement. This is further illustrated in Fig. 7, which plots the maximum surface energy change required to shift liquid-metal slugs of varying length from one minimum-energy position to the next for channels with different diameter-to-spacing ratios.

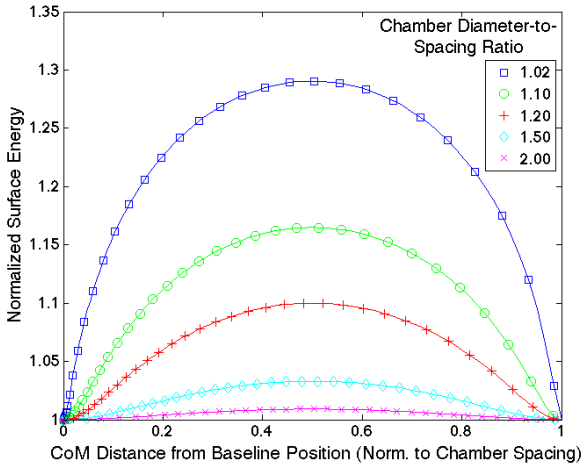

FIGURE 6. Normalized change in surface energy as a liquid-metal slug ($N = 1$) moves between adjacent chambers.

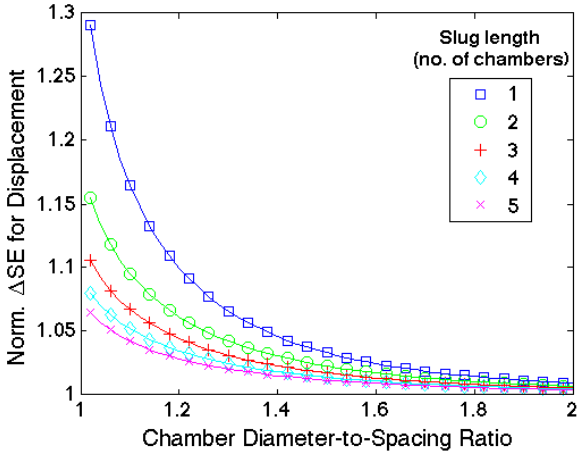

FIGURE 7. Normalized change in surface energy required for displacement of a liquid-metal slug from one minimum-energy position to the next for channels of varying geometry. Low diameter-to-spacing ratios result in narrow openings and greater deformation of the liquid metal, whereas higher ratios more closely resemble uniform rectangular channels and require little additional energy. Longer slugs have higher baseline energy states and require less additional energy for displacement.

While chambers spaced further apart will increase the additional surface energy required to move the liquid metal regardless of length, it can be seen that this effect is reduced for longer slugs as these have higher baseline surface energy levels as described by (4). The correspondingly lower maximum-to-minimum surface energy ratios make it relatively easier for longer slugs to become displaced, although in practice the high surface tension of Galinstan and other liquid metals makes it very difficult for the slug to maintain any configuration that does not minimize its surface area.

While channels with lower diameter-to-spacing ratios are more effective at holding the liquid metal in place after actuation due to the larger maximum-to-minimum surface energy ratios, these channels also result in very narrow openings between chambers, making actuation more difficult. Alternately, chambers that are more closely spaced together can result in higher-fidelity position control, but for a given chamber radius this also increases the diameter-to-spacing ratio to the point that the slug can be unintentionally displaced from its intended location. The authors have empirically found a diameter-to-spacing ratio of 1.2 to be a good balance between reliable actuation and dependable positioning control, allowing for a typical repeatability of less than 500 μm for a slug's intended resting position. This empirical value is supported by the analytical data in Fig. 7, which, while varying slightly based on slug length, shows a sharp increase in required surface energy for diameter-to-spacing ratios below approximately 1.15 as well as diminishing returns for ratios above approximately 1.2.

IV. PROTOTYPE DEVICE

To demonstrate the feasibility of using the actuation and positioning concepts presented above to integrate non-toxic liquid metal as a tuning element in an RF device, a prototype was fabricated that utilizes liquid metal as a means of dynamically altering its performance. For this purpose we have chosen a slot antenna, both for its popularity in radar and satellite communication applications as well as for the simplicity in both its fabrication and operating principles. This simplicity helps to emphasize that the techniques demonstrated here can be easily exported to other RF devices.

A. THEORY OF OPERATION

The prototype slot antenna is center-fed by a microstrip on the opposite side of a dielectric substrate. Energy from the microstrip is coupled onto the aperture, resulting in quasi-TE waves propagating along the slotline [31] from the center of the aperture to the short circuits at either end. When the electrical length of the slotline is roughly equal to half of a guided wavelength of the driving signal, the aperture will radiate in a manner analogous to a dipole antenna.

The resonant frequency of the slot antenna can be altered via reactive loading, which can be accomplished by changing the length of the microstrip line as it extends beyond the aperture. This is equivalent to placing an open-circuit tuning stub in series with the complex impedance presented to the source by the aperture [32]. The reactance presented by the tuning stub, assuming negligible transmission line loss, is $-jZ_{o,f}\,cot(\beta d)$, where $Z_{o,f}$ is the characteristic impedance of the feed stub, β is the wavenumber, and d is the length of the stub as it extends beyond the aperture. Thus, by varying the extent of the feed line d, reactance can be added to or subtracted from the system, loading the antenna and shifting its resonant frequency. Previous research has demonstrated the feasibility of this approach by varying the electrical length of the feed line with nonlinear components [33], [34].

The slot antenna presented here achieves frequency tunability by utilizing a hybrid microstrip feed composed of a conventional copper trace capacitively coupled to a liquid-metal slug resting in a channel above the microstrip. By shifting the position of the liquid metal, the electrical length of the feed line is altered, which in turn

reactively loads the antenna and shifts its resonant frequency. CEW actuation allows for this tuning to be accomplished electronically, and the process is made repeatable through the use of interlocking circular chambers that dictate the discrete positions at which the liquid-metal element can minimize its surface energy.

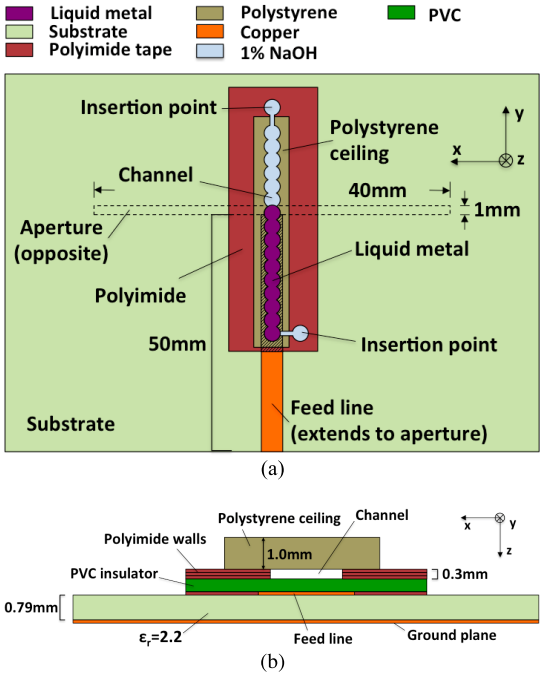

FIGURE 8. Topology of the liquid-metal feed slot antenna: (a) top and (b) side view.

B. FABRICATION AND TEST

The hybrid liquid-metal feed slot antenna (Fig. 8) is fabricated on a 10 cm × 7 cm dielectric substrate with a thickness of 0.787 mm and a relative permittivity of 2.2. On one side of the substrate is a copper ground plane with a 40 mm × 1 mm rectangular aperture. The aperture is center-fed on the opposite side of the substrate by a 2.4-mm-wide microstrip line that extends up to, but not across, the aperture.

On top of the copper microstrip feed line is a hollow polyimide channel containing both the liquid metal as well as the encompassing electrolyte (1% NaOH). The channel is comprised of interconnected circular chambers that are spaced 1.5 mm apart (center-to-center) with a diameter of 1.8 mm. The channel is 300 μm high and is isolated from the copper line to prevent an alloying reaction between the Galinstan and copper. This isolation necessitates that the coupling between the copper feed and the Galinstan be purely capacitive; to maximize coupling the channel is designed so that no less than 30% of the liquid-metal slug is always situated directly over the copper feed, providing a low-impedance RF path. The channel is capped by a 1-mm-thick layer of polystyrene, which provides structural support.

The channel is initially filled with the electrolytic carrier fluid, after which a liquid-metal slug filling the first

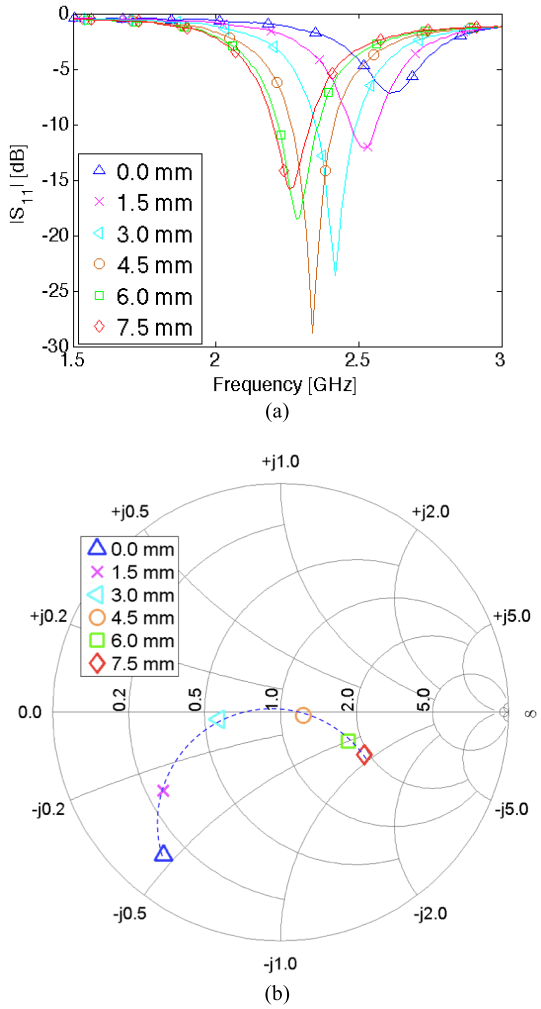

FIGURE 9. (a) S_{11} and (b) input impedance results for the extension of the liquid-metal feed beyond the aperture.

10 chambers (i.e. 15.3 mm long) is injected into the channel. The slug originally rests over the copper microstrip line, extending up to the far edge of the aperture, but not beyond. By applying a square-wave actuation signal (8 Vpp, +3 VDC offset, 30 Hz), CEW actuation is initiated and the liquid-metal slug begins moving beyond the aperture, effectively extending the copper feed line and reactively loading the antenna. When the actuation signal is removed, the liquid metal minimizes its surface energy by filling the circular chambers it now occupies, falling into one of six minimum-energy positions. Reversing the polarity of the DC bias reverses the process, and because the carrier fluid chemically reduces the oxide layer of the Galinstan slug, the user is able to change the length of the feed line between these states immediately and reversibly without having to clean the channel out between uses, as in [27]. It is important to note that this is a low-voltage and low-power process, requiring only 8 V_{pp} and less than 10 mW for actuation. By contrast, the micropump used to hydraulically actuate liquid metal in [35] requires voltages between 100 and 250 V and has a power consumption of up to 200 mW [36].

S_{11} measurements for the prototype slot antenna are shown in Fig. 9, along with the input impedance of the antenna at its approximate center frequency of 2.35 GHz. The effective tunable bandwidth of the antenna, or the frequency range over which the return loss is greater than 10 dB, is 15.2%. As the liquid metal is extended further beyond the aperture, the input impedance rotates clockwise around a translated circle of constant resistance, as it would for an increasingly long open-circuit microstrip stub. This demonstrates that the liquid metal is behaving as part of a dynamic signal transmission line whose length can be varied with low-power electrical signals. Multiple measurements taken at each discrete state yield the same results, confirming the accuracy with which the resting position of the liquid metal can be controlled as well as the high degree of repeatability that can be achieved with liquid-metal tuning.

During actuation, the impedance mismatch presented by the presence of the lossy electrolyte can interfere with the intended operation of the tuning stub, and in this case can also hamper antenna efficiency (the peak gain for this prototype antenna was approximately 2 dBi, down from 5-6 dBi for a baseline copper-only version). This is a drawback to the use of water-based electrolytes in RF applications, and may be mitigated in the future through either the use of a lower-loss electrolyte, or by careful design that minimizes the proximity of the electrolyte to the RF signal.

V. CONCLUSION

This paper discussed the advantages of utilizing a non-toxic liquid metal alloy as a tuning element in an RF device, and proposed solutions to two of the biggest challenges involved in this implementation. Reliable actuation of the liquid metal can be achieved by applying a square wave with a DC bias, which alternates between propelling the slug forward and limiting the re-growth of the oxide layer on the slug's trailing edge. The slug's position can be controlled by providing the liquid metal with discrete positions of minimum surface energy within the channel, taking advantage of the high surface tension of the liquid metal. Both of these techniques are used to create a microstrip feedline whose electrical length can be controlled via low-power electronic actuation; this line is used to reactively load a slot antenna, varying its resonant frequency over a 15.2% bandwidth. Through the refinement of these and similar techniques, we believe that there is great promise in using liquid metal to create dynamic, reconfigurable RF devices.

REFERENCES

[1] X. Artiga, J. Perruisseau-Carrier, P. Pardo-Carrera, I. Llamas-Garro, and Z. Brito-Brito, "Halved Vivaldi antenna with reconfigurable band rejection," *IEEE Antennas Wireless Propag. Lett.*, vol. 10, pp. 56–58, 2011.

[2] S. V. Hum and H. Y. Xiong, "Analysis and design of a differentially-fed frequency agile microstrip patch antenna," *IEEE Trans. Antennas Propag.*, vol. 58, no. 10, pp. 3122–3130, Oct. 2010.

[3] M. Jusoh, T. Sabapathy, M. F. Jamlos, and M. R. Kamarudin, "Reconfigurable four-parasitic-elements patch antenna for high-gain beam switching application," *IEEE Antennas Wireless Propag. Lett.*, vol. 13, pp. 79–82, 2014.

[4] J. T. Rayno and S. K. Sharma, "Wideband frequency-reconfigurable spirograph planar monopole antenna (SPMA) operating in the UHF band," *IEEE Antennas Wireless Propag. Lett.*, vol. 11, pp. 1537–1540, 2012.

[5] M. A. El-Tanani and G. M. Rebeiz, "High-performance 1.5–2.5-GHz RF-MEMS tunable filters for wireless applications," *IEEE Trans. Microw. Theory Techn.*, vol. 58, no. 6, pp. 1629–1637, Jun. 2010.

[6] A. Zohur, H. Mopidevi, D. Rodrigo, M. Unlu, L. Jofre, and B. A. Cetiner, "RF MEMS reconfigurable two-band antenna," *IEEE Antennas Wireless Propag. Lett.*, vol. 12, pp. 72–75, 2013.

[7] T. Liu, P. Sen, and C.-J. Kim, "Characterization of nontoxic liquid-metal alloy Galinstan for applications in microdevices," *J. Microelectromech. Syst.*, vol. 21, no. 2, pp. 443–450, Apr. 2012.

[8] M. Kelley *et al.*, "Frequency reconfigurable patch antenna using liquid metal as switching mechanism," *Electron. Lett.*, vol. 49, no. 22, pp. 1370–1371, Oct. 2013.

[9] S. Cheng, Z. Wu, P. Hallbjorner, K. Hjort, and A. Rydberg, "Foldable and stretchable liquid metal planar inverted cone antenna," *IEEE Trans. Antennas Propag.*, vol. 57, no. 12, pp. 3765–3771, Dec. 2009.

[10] M. Kubo *et al.*, "Stretchable microfluidic radiofrequency antennas," *Adv. Mater.*, vol. 22, no. 25, pp. 2749–52, Jul. 2010.

[11] G. J. Hayes, J.-H. So, A. Qusba, M. D. Dickey, and G. Lazzi, "Flexible liquid metal alloy (EGaIn) microstrip patch antenna," *IEEE Trans. Antennas Propag.*, vol. 60, no. 5, pp. 2151–2156, May 2012.

[12] G. Mumcu, A. Dey, and T. Palomo, "Frequency-agile bandpass filters using liquid metal tunable broadside coupled split ring resonators," *IEEE Microw. Wireless Compon. Lett.*, vol. 23, no. 4, pp. 187–189, Apr. 2013.

[13] C.-H. Chen, J. Whalen, and D. Peroulis, "Non-toxic liquid-metal 2–100 GHz MEMS switch," in *IEEE/MTT-S Int. Microw. Symp. Dig.*, Honolulu, HI, USA, Jun. 2007, pp. 363–366.

[14] W. Irshad and D. Peroulis, "A 12–18 GHz electrostatically tunable liquid metal RF MEMS resonator with quality factor of 1400–1840," in *IEEE MTT-S Int. Microw. Symp. Dig.*, Baltimore, MD, USA, Jun. 2011, pp. 1–4.

[15] A. M. Morishita, C. K. Y. Kitamura, A. T. Ohta, and W. A. Shiroma, "A liquid-metal monopole array with tunable frequency, gain, and beam steering," *IEEE Antennas Wireless Propag. Lett.*, vol. 12, pp. 1388–1391, 2013.

[16] M. Li and N. Behdad, "Fluidically tunable frequency selective/phase shifting surfaces for high-power microwave applications," *IEEE Trans. Antennas Propag.*, vol. 60, no. 6, pp. 2748–2759, Jun. 2012.

[17] Y. Damgaci and B. A. Cetiner, "A frequency reconfigurable antenna based on digital microfluidics," *Lab Chip*, vol. 13, no. 15, pp. 2883–2887, Aug. 2013.

[18] H. J. Lee and C.-J. Kim, "Surface-tension-driven microactuation based on continuous electrowetting," *J. Microelectromech. Syst.*, vol. 9, no. 2, pp. 171–180, Jun. 2000.

[19] K.-S. Yun *et al.*, "A micropump driven by continuous electrowetting actuation for low voltage and low power operations," in *Proc. 14th IEEE Int. Conf. Micro Electro Mech. Syst. (MEMS)*, Jan. 2001, pp. 487–490.

[20] J. L. Jackel, S. Hackwood, J. J. Veselka, and G. Beni, "Electrowetting switch for multimode optical fibers," *Appl. Opt.*, vol. 22, no. 11, pp. 1765–1770, Jun. 1983.

[21] G. Beni, "Continuous electrowetting effect," *Appl. Phys. Lett.*, vol. 40, no. 10, pp. 912–914, 1982.

[22] J. Lee and C.-J. C. Kim, "Theory and modeling of continuous electrowetting microactuation," in *Proc. ASME Int. Mech. Eng. Congr. Exposit. (MEMS)*, 1999, pp. 397–403.

[23] S.-Y. Tang *et al.*, "Electrochemically induced actuation of liquid metal marbles," *Nanoscale*, vol. 5, no. 13, pp. 5949–5957, Jul. 2013.

[24] S.-Y. Tang *et al.*, "Liquid metal enabled pump," *Proc. Nat. Acad. Sci. USA*, vol. 111, no. 9, pp. 3304–3309, Mar. 2014.

[25] T. B. Jones, "An electromechanical interpretation of electrowetting," *J. Micromech. Microeng.*, vol. 15, no. 6, pp. 1184–1187, Jun. 2005.

[26] E. Baird, P. Young, and K. Mohseni, "Electrostatic force calculation for an EWOD-actuated droplet," *Microfluidics Nanofluidics*, vol. 3, no. 6, pp. 635–644, Jan. 2007.

[27] A. J. King, J. F. Patrick, N. R. Sottos, S. R. White, G. H. Huff, and J. T. Bernhard, "Microfluidically switched frequency-reconfigurable slot antennas," *IEEE Antennas Wireless Propag. Lett.*, vol. 12, pp. 828–831, 2013.

[28] R. C. Gough, J. H. Dang, A. M. Morishita, A. T. Ohta, and W. A. Shiroma, "Frequency-tunable slot antenna using continuous electrowetting of liquid metal," in *IEEE MTT-S Int. Microw. Symp. Dig.*, Tampa, FL, USA, Jun. 2014, pp. 1–3.

[29] D. Zrnic and D. Swatik, "On the resistivity and surface tension of the eutectic alloy of gallium and indium," *J. Less Common Met.*, vol. 18, no. 1, pp. 67–68, May 1969.
[30] B. Lautrup, "Chapter 5: Surface tension," in *Physics of Continuous Matter*, 2nd ed. Boca Raton, FL, USA: CRC Press, 2011, pp. 69–94.
[31] K. C. Gupta, R. Garg, and I. J. Bahl, "Slotlines I: Analyses and design considerations," in *Microstrip Lines and Slotlines*, 1st ed. Dedham, MA, USA: Artech House, 1979, pp. 195–229.
[32] D. M. Pozar, "A reciprocity method of analysis for printed slot and slot-coupled microstrip antennas," *IEEE Trans. Antennas Propag.*, vol. 34, no. 12, pp. 1439–1446, Dec. 1986.
[33] I. Carrasquillo-Rivera, Z. Popovic, and R. A. R. Solis, "Tunable slot antenna using varactors and photodiodes," in *IEEE Antennas Propag. Soc. Int. Symp. Dig.*, vol. 4. Jun. 2003, pp. 532–535.
[34] A. Valizade, C. Ghobadi, J. Nourinia, and M. Ojaroudi, "A novel design of reconfigurable slot antenna with switchable band notch and multiresonance functions for UWB applications," *IEEE Antennas Wireless Propag. Lett.*, vol. 11, pp. 1166–1169, 2012.
[35] D. Rodrigo, L. Jofre, and B. A. Cetiner, "Circular beam-steering reconfigurable antenna with liquid metal parasitics," *IEEE Trans. Antennas Propag.*, vol. 60, no. 4, pp. 1796–1802, Apr. 2012.
[36] *Bartels Micropumps*, Bartels Mikrotechnik GmbH, Dortmund, Germany, May 2014, p. 7.

RYAN C. GOUGH (S'13) received the B.S. degree in electrical engineering from Texas Tech University, Lubbock, TX, USA, in 2006, and the M.S. degree in electrical engineering from Southern Methodist University, Dallas, TX, USA, in 2010. He is currently pursuing the Ph.D. degree in electrical engineering with the University of Hawai'i at Mānoa, Honolulu, HI, USA, where his research focuses on the electrical actuation of liquid metal for use in reconfigurable RF electronics.

He was an RF Engineer with Lockheed Martin Aeronautics Company (LMAC), Fort Worth, TX, USA, from 2006 to 2011, where he was involved in electromagnetic compatibility testing and production-level antenna characterization. In 2008, he was one of the 25 young engineers selected company-wide for participation in the LMAC Engineering Leadership Development Program, designed to identify and develop future engineering leaders.

Mr. Gough was named the 2014 Scholar of the Year by the Honolulu Chapter of the Achievement Rewards for College Scientists (ARCS) Foundation, and is the Chair of the University of Hawai'i at Mānoa's Student Branch Chapter of the IEEE Microwave Theory and Techniques Society (MTT-S). His paper on dynamic aperture slot antennas was awarded Second Place in the Student Paper Competition of the 2014 IEEE MTT-S International Microwave Symposium.

ANDY M. MORISHITA (S'11) received the B.S. degree in electrical engineering from the University of Hawai'i at Mānoa, Honolulu, HI, USA, in 2012, where he is currently pursuing the M.S. degree in electrical engineering.

He joined the Microwave/Millimeter-Wave Research Laboratory, University of Hawai'i at Mānoa, in 2012. He has authored seven publications. His research interests include reconfigurable architectures, microwave circuits, and antennas.

Mr. Morishita was the Founding Chair of the University of Hawai'i at Mānoa's Student Branch Chapter of the IEEE Microwave Theory and Techniques Society (MTT-S). He was a recipient of the University of Hawai'i College of Engineering's 2014 Outstanding M.S. Research Award and the 2014 IEEE MTT-S Pre-Graduate Scholarship Award.

JONATHAN H. DANG (S'10) received the B.S. degree in electrical engineering from the University of Hawai'i at Mānoa, Honolulu, HI, USA, in 2013, where he is currently pursuing the M.S. degree in electrical engineering.

He joined the Microwave/Millimeter-Wave Research Laboratory, University of Hawai'i at Mānoa, in 2013. He has authored five publications. His research interests include robotics, microwave circuits, and embedded software development.

Mr. Dang was a recipient of the 2013 Student Engineer of the Year Award from the Hawai'i Council of Engineering Societies, and the 2014–2015 IEEE Life Members Graduate Study Fellowship in Electrical Engineering.

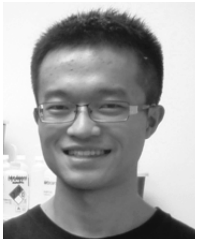

WENQI HU (S'10) received the B.S. degree in electrical engineering from the University of Electronic Science and Technology of China, Chengdu, China, in 2005, and the Ph.D. degree in electrical engineering from the University of Hawai'i at Mānoa, Honolulu, HI, USA, in 2014.

He is currently a Post-Doctoral Researcher with the Max Planck Institute for Intelligent Systems, Stuttgart, Germany. He has authored 19 publications. His research interests include microrobotics and biomedical microtools for tissue engineering.

Dr. Hu was a recipient of the University of Hawai'i College of Engineering's 2014 Outstanding Ph.D. Research Award. He was also a finalist for the Best Conference Paper Award at the 2012 IEEE International Conference on Robotics and Automation.

WAYNE A. SHIROMA (S'85–M'87–SM'08) received the B.S. degree from the University of Hawai'i at Mānoa, Honolulu, HI, USA, in 1986, the M.Eng. degree from Cornell University, Ithaca, NY, USA, in 1987, and the Ph.D. degree from the University of Colorado at Boulder, Boulder, CO, USA, in 1996, all in electrical engineering.

He joined the University of Hawai'i at Mānoa, in 1996, where he is currently a Professor and the Chair of Electrical Engineering. He has authored over 100 publications in the areas of microwave circuits and antennas, nanosatellites, and engineering education. He was also a member of the technical staff with Hughes Space and Communications, El Segundo, CA, USA.

Dr. Shiroma served three terms on the IEEE Microwave Theory and Techniques Society (MTT-S) Administrative Committee, from 2002 to 2010, and was the General Chair of the 2007 IEEE MTT-S International Microwave Symposium. He was a recipient of the 2003 University of Hawai'i (UH) Regent's Medal for Excellence in Teaching, the ten-campus UH System's most prestigious teaching award. Since 2001, IEEE-HKN, the international honor society for IEEE, recognized four of his graduating seniors as the most outstanding electrical engineering students in the U.S.

AARON T. OHTA (S'99–M'09) received the B.S. degree from the University of Hawai'i at Mānoa, Honolulu, HI, USA, in 2003, the M.S. degree from the University of California at Los Angeles, Los Angeles, CA, USA, in 2004, and the Ph.D. degree from the University of California at Berkeley, Berkeley, CA, USA, in 2008, all in electrical engineering.

He joined the University of Hawai'i at Mānoa, in 2009, where he is currently an Associate Professor of Electrical Engineering. He has authored over 80 publications in the areas of microelectromechanical systems and microfluidics.

Dr. Ohta was a recipient of the 2012 University of Hawai'i (UH) Regent's Medal for Excellence in Research, the ten-campus UH System's most prestigious research award.